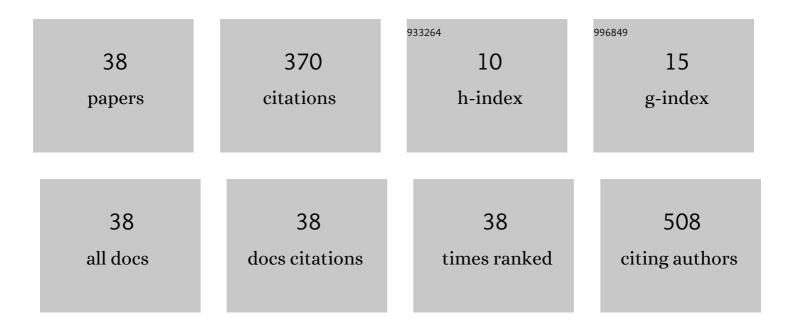
Zebin Xiao

List of Publications by Year in descending order

Source: https://exaly.com/author-pdf/3981385/publications.pdf Version: 2024-02-01



ZERIN XIAO

#	Article	IF	CITATIONS
1	Dual-energy CT in differentiating benign sinonasal lesions from malignant ones: comparison with simulated single-energy CT, conventional MRI, and DWI. European Radiology, 2022, 32, 1095-1105.	2.3	12
2	Extramedullary Plasmacytoma of the Sinonasal Cavity: Magnetic Resonance Imaging Characteristics With Readout-Segmented Diffusion-Weighted Imaging and Dual-Energy Computed Tomography Features. Journal of Computer Assisted Tomography, 2022, 46, 264-268.	0.5	1
3	Metabolic alterations in the visual pathway of retinitis pigmentosa rats: A longitudinal multimodal magnetic resonance imaging study with histopathological validation. NMR in Biomedicine, 2022, 35, .	1.6	3
4	Altered spontaneous neuronal activity and functional connectivity pattern in primary angle-closure glaucoma: a resting-state fMRI study. Neurological Sciences, 2021, 42, 243-251.	0.9	13
5	Nicotinamide ameliorates energy deficiency and improves retinal function in Cavâ€1 ^{â€/â€} mice. Journal of Neurochemistry, 2021, 157, 550-560.	2.1	8
6	Imaging of T-cell Responses in the Context of Cancer Immunotherapy. Cancer Immunology Research, 2021, 9, 490-502.	1.6	8
7	Dual-energy CT in predicting Ki-67 expression in laryngeal squamous cell carcinoma. European Journal of Radiology, 2021, 140, 109774.	1.2	11
8	Magnetic resonance imaging investigations reveal that PM2.5 exposure triggers visual dysfunction in mice. Ecotoxicology and Environmental Safety, 2021, 227, 112866.	2.9	4
9	White Matter Alterations in Spastic Paraplegia Type 5: A Multiparametric Structural MRI Study and Correlations with Biochemical Measurements. American Journal of Neuroradiology, 2021, , .	1.2	0
10	Wholeâ€ŧumor histogram analysis of monoexponential and advanced diffusionâ€weighted imaging for sinonasal malignant tumors: Correlations with histopathologic features. Journal of Magnetic Resonance Imaging, 2020, 51, 273-285.	1.9	16
11	Diffusion Kurtosis Imaging and Intravoxel Incoherent Motion in Differentiating Nasal Malignancies. Laryngoscope, 2020, 130, E727-E735.	1.1	4
12	Therapeutic Targeting of Retinal Immune Microenvironment With CSF-1 Receptor Antibody Promotes Visual Function Recovery After Ischemic Optic Neuropathy. Frontiers in Immunology, 2020, 11, 585918.	2.2	16
13	Comparison of Conventional, Diffusion, and Perfusion MRI Between Low-Grade and Anaplastic Extraventricular Ependymoma. American Journal of Roentgenology, 2020, 215, 978-984.	1.0	2
14	Performance of diffusion and perfusion MRI in evaluating primary central nervous system lymphomas of different locations. BMC Medical Imaging, 2020, 20, 62.	1.4	1
15	Dual-energy CT in the differentiation of stage T1 nasopharyngeal carcinoma and lymphoid hyperplasia. European Journal of Radiology, 2020, 124, 108824.	1.2	12
16	Benign and malignant skull-involved lesions: discriminative value of conventional CT and MRI combined with diffusion-weighted MRI. Acta Radiologica, 2019, 60, 880-886.	0.5	7
17	Differentiation between sinonasal natural killer/T-cell lymphomas and diffuse large B-cell lymphomas by RESOLVE DWI combined with conventional MRI. Magnetic Resonance Imaging, 2019, 62, 10-17.	1.0	8
18	Manganese-enhanced magnetic resonance imaging in the whole visual pathway: chemical identification and neurotoxic changes. Acta Radiologica, 2019, 60, 1653-1662.	0.5	2

ZEBIN XIAO

#	Article	IF	CITATIONS
19	Evaluation of hyperbaric oxygen therapy for spinal cord injury in rats with different treatment course using diffusion tensor imaging. Spinal Cord, 2019, 57, 404-411.	0.9	4
20	CT, conventional, and functional MRI features of skull lymphoma: a series of eight cases in a single institution. Skeletal Radiology, 2019, 48, 897-905.	1.2	6
21	Differentiation between benign and malignant palatal tumors using conventional MRI: a retrospective analysis of 130 cases. Oral Surgery, Oral Medicine, Oral Pathology and Oral Radiology, 2018, 125, 343-350.	0.2	16
22	Hepatocellular Carcinoma: Retrospective Evaluation of the Correlation Between Gadobenate Dimeglumine–Enhanced Magnetic Resonance Imaging and Pathologic Grade. Journal of Computer Assisted Tomography, 2018, 42, 365-372.	0.5	6
23	Intravoxel Incoherent Motion MR Imaging in the Differentiation of Benign and Malignant Sinonasal Lesions: Comparison with Conventional Diffusion-Weighted MR Imaging. American Journal of Neuroradiology, 2018, 39, 538-546.	1.2	16
24	Standard diffusion-weighted, diffusion kurtosis and intravoxel incoherent motion MR imaging of sinonasal malignancies: correlations with Ki-67 proliferation status. European Radiology, 2018, 28, 2923-2933.	2.3	45
25	Differentiation of olfactory neuroblastomas from nasal squamous cell carcinomas using MR diffusion kurtosis imaging and dynamic contrastâ€enhanced MRI. Journal of Magnetic Resonance Imaging, 2018, 47, 354-361.	1.9	16
26	Differentiating between benign and malignant sinonasal lesions using dynamic contrast-enhanced MRI and intravoxel incoherent motion. European Journal of Radiology, 2018, 98, 7-13.	1.2	16
27	Diffusion-weighted MRI combined with susceptibility-weighted MRI: added diagnostic value for four common lateral ventricular tumors. Acta Radiologica, 2018, 59, 980-987.	0.5	5
28	Metabolic Alterations Within the Primary Visual Cortex in Early Open-angle Glaucoma Patients: A Proton Magnetic Resonance Spectroscopy Study. Journal of Glaucoma, 2018, 27, 1046-1051.	0.8	6
29	White Matter Abnormalities and Correlation With Severity in Normal Tension Glaucoma: A Whole Brain Atlas-Based Diffusion Tensor Study. , 2018, 59, 1313.		32
30	Visual cortex and auditory cortex activation in early binocularly blind macaques: A BOLD-fMRI study using auditory stimuli. Biochemical and Biophysical Research Communications, 2017, 485, 796-801.	1.0	4
31	Evaluation of changes in magnetic resonance diffusion tensor imaging of the bilateral optic tract in monocular blind rats. International Journal of Developmental Neuroscience, 2017, 59, 10-14.	0.7	2
32	IDH mutant and 1p/19q co-deleted oligodendrogliomas: tumor grade stratification using diffusion-, susceptibility-, and perfusion-weighted MRI. Neuroradiology, 2017, 59, 555-562.	1.1	36
33	Manganeseâ€enhanced magnetic resonance imaging combined with electrophysiology in the evaluation of visual pathway in experimental rat models with monocular blindness. Brain and Behavior, 2017, 7, e00731.	1.0	5
34	Manganeseâ€enhanced MR imaging (MEMRI) combined with electrophysiology in the study of crossâ€modal plasticity in binocularly blind rats. International Journal of Developmental Neuroscience, 2017, 61, 12-20.	0.7	2
35	Manganeseâ€enhanced MRI (MEÂMRI) in evaluation of the auditory pathway in an experimental rat model. NMR in Biomedicine, 2017, 30, e3677.	1.6	4
36	Four-dimensional CT angiography (4D-CTA) in the evaluation of juvenile nasopharyngeal angiofibromas: comparison with digital subtraction angiography (DSA) and surgical findings. Dentomaxillofacial Radiology, 2017, 46, 20170171.	1.3	5

#	Article	IF	CITATIONS
37	Assessment of severity of leukoaraiosis: a diffusional kurtosis imaging study. Clinical Imaging, 2016, 40, 732-738.	0.8	6
38	Multiple paragangliomas of head and neck associated with hepatic paraganglioma: a case report. BMC Medical Imaging, 2015, 15, 38.	1.4	10